Geoscientific
Model Development
Discussions

Open Access

EGU

INFERNO: a fire and emissions scheme for the Met Office's Unified Model

Stephane Mangeon[1,2], Apostolos Voulgarakis[1], Richard Gilham[2], Anna Harper[3], Stephen Sitch[4], Gerd Folberth[2]

[1]Department of Physics, Imperial College London, London, United Kingdom
[2]Met Office, FitzRoy Road, Exeter, EX1 3PB, UK
[3]College of Engineering, Mathematics, and Physical Sciences, University of Exeter, Exeter, UK
[4]College of Life and Environmental Sciences, University of Exeter, Exeter, UK

Correspondence to: Stéphane Mangeon (stephane.mangeon12@imperial.ac.uk)

Abstract. Warm and dry climatological conditions favour the occurrence of forest fires. These fires then become a significant emission source to the atmosphere. Despite this global importance, fires are a local phenomenon and are difficult to represent in a large-scale Earth System Model (ESM). To address this, the INteractive Fire and Emission algoRithm for Natural envirOnments (INFERNO) was developed. INFERNO follows a reduced complexity approach and is intended for decadal to centennial scale climate simulations and assessment models for policy making. Fuel flammability is simulated using temperature, relative humidity, fuel density as well as precipitation and soil moisture. Combining flammability with ignitions and vegetation, burnt area is diagnosed. Emissions of carbon and key species are estimated using the carbon scheme in the JULES land surface model. JULES also possesses fire index diagnostics which we document and compare with our fire scheme. Two meteorology datasets and three ignition modes are used to validate the model. INFERNO is shown to effectively diagnose global fire occurrence (R=0.66) and emissions (R=0.59) through an approach appropriate to the complexity of an ESM, although regional biases remain.

1 Introduction

Fire is a key interaction between the atmosphere and the land surface (Bowman et al., 2009). Its impacts are wide-ranging: it influences forest succession (Bond and Keeley, 2005), is a tool for deforestation (van der Werf et al., 2009) and is an important natural carbon source (Bowman et al., 2013), while it also provides a major natural hazard to humans through property and infrastructure destruction and air quality degradation (Johnston et al., 2012; Marlier et al., 2013). Not only are biomass burning emissions substantial in magnitude (Lamarque et al., 2010), they also drive the variability of atmospheric composition (Spracklen et al., 2007; Voulgarakis et al., 2010, 2015) and impact short-term climate forcing (Tosca et al., 2013).

There are feedbacks between fire and climate: low-humidity conditions cause droughts, which enhance fire activity (Field et al., 2009), which, in turn, emits aerosols and trace gases (Akagi et al., 2011), influencing the abundances of radiatively active atmospheric constituents, cloud formation and lifetime, and in turn precipitation, and surface albedo (Voulgarakis and Field, 2015). Bistinas et al. (2014) showed global fire frequency is correlated with land-use, vegetation type and meteorological factors (dry days, soil moisture and maximum temperature) and human presence tends to noticeably reduce fire activity (land-management, landscape fragmentation and urbanization). Examining and quantifying such impacts and feedbacks is paramount to Earth System Models (ESMs), yet to integrate vegetation fires presents many challenges as it intricately links multiple disciplines from ecology to atmospheric chemistry and physics and climate science.

Integration of fires into Dynamic Global Vegetation Models (DGVMs) was the first step towards fire within ESMs (e.g. (Arora and Boer, 2005; Fosberg et al., 1999; Li et al., 2012; Pfeiffer et al., 2013; Sitch et al., 2003; Thonicke et al., 2001, 2010; Venevsky et al., 2002; Yue et al., 2014). Vegetation fires have been implemented into only a few ESMs, e.g. ECHAM (Lasslop et al., 2014) and the Community ESM (Li et al., 2013, 2014, p.2).

Here, we present and evaluate the INteractive Fire and Emission algoRithm for Natural envirOnments (INFERNO) and its implementation. INFERNO is a necessarily simple parameterization that focuses on the large-scale occurrence of fires and is suitable for ESM application. The model uses a few key driving variables while retaining a broadly accurate parameterization for fire emissions. INFERNO's performance against observations and well established and operationally relevant fire indices is presented.

2 Model description

2.1 INFERNO

INFERNO was constructed upon the simplified parameterization for fire counts proposed and evaluated for the present-day by (Pechony and Shindell, 2009), which was subsequently shown to provide a good estimate for large-scale fire variability over climatological timescales (Pechony and Shindell, 2010). In short, that parameterization used monthly mean temperature, relative humidity and precipitation to simulate fuel flammability. It also used human population density and lightning to represent ignitions. To incorporate this parameterization within the Joint UK Land Environment Simulator (JULES, Best et

Geoscientific
Model Development
Discussions

62   al., 2011; Clark et al., 2011), several changes were applied. Upper layer soil moisture is used to represent

63   precipitation memory while precipitation acts as a rapid fire deterrent. Vegetation Density was replaced

64   by Fuel Density, an index dependent on leaf carbon and Decomposable Plant Material (DPM), i.e. litter.

65   Such a relationship with fine fuel and moisture was used in Thonicke et al. (2001). Furthermore, we

66   developed a parameterization to obtain burnt area (BA), emitted carbon (EC) and fire emissions of

67   different species (E_X) and our fire diagnostics are made for each of the nine Plant Functional Types

68   (PFTs) in the current version of JULES (Harper et al., submitted).

69   Figure 1 summarizes the mechanisms of INFERNO, and Fig. A1 illustrates the dependence of INFERNO
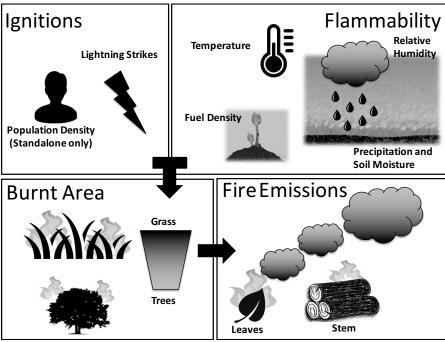
70   on individual driving variables.

71

72   **Fig. 1. Schematic summarizing the INteractive Fire and Emission algoRithm for Natural envirOnments**
73   **(INFERNO) and its key components and behaviour. Ignitions can be accounted for in a variety of ways (see**
74   **Sect. 2.1.1), meteorology influences flammability (see Sect. 2.1.2), while plant coverage influences burnt area**
75   **(see Sect. 2.1.3), finally emissions are calculated according to leaf and stem carbon for each PFT (see Sect.**
76   **2.1.4).**

77   **2.1.1 Ignitions (*I*)**

78   INFERNO calculates ignitions in either one of three modes:

79   First, we can assume constant or ubiquitous ignitions, currently calibrated to a global average of $I_T =$

80   1.67 ignitions km^{-2} $month^{-1}$. This corresponds to 1.5 ignitions km^{-2} $month^{-1}$ due to humans (I_A),

81   heuristically determined, and 0.17 ignitions km^{-2} $month^{-1}$ natural ignitions due to lightning (I_N), derived

82   from the multi-year annual mean of 2.7 strikes km^{-2} $year^{-1}$ (Huntrieser et al., 2007) assuming 75% of

83   strikes being cloud-to-ground (Prentice and Mackerras, 1977). This mode inherently suppresses the

84   variability in fires due to any anthropogenic or natural ignition changes (Pechony and Shindell, 2009,

85   2010).

Geoscientific
Model Development
Discussions

86   Second, human ignitions and suppressions can be assumed to remain constant at the global mean value

87   mentioned above ($I_A = 1.5$ ignitions km^{-2} month^{-1}), however cloud-to-ground lightning strikes may vary,

88   and in addition each strike is assumed to start a fire. This mode accounts for natural variability in fire

89   ignitions, which can be simulated within an ESM, or prescribed from observations.

90   Third, varying human ignitions and suppressions and varying natural ignitions (cloud-to-ground

91   lightning strikes, as in mode 2). This was the original ignition approach in Pechony and Shindell (2009),

92   which was left unchanged and is detailed below. In this ignition mode, anthropogenic ignition and

93   suppression depends on population density (PD), as proposed by Venevsky et al. (2002).

94    $$I_A = k(PD)\, PD\, \alpha \qquad (1)$$

95   PD is in units of people km^{-2}, and $k(PD) = 6.8 \times PD^{-0.6}$ is a function that represents the varying

96   anthropogenic influence on ignitions in rural versus urban environments. The parameter $\alpha = 0.03$

97   represents the number of potential ignition sources per person per month per km^2. Both natural and

98   anthropogenic ignitions have the potential to be suppressed by humans, such that the fraction of fires not

99   suppressed is:

100    $$f_{NS} = 7.7\,(0.05 + 0.9 \times e^{-0.05\,PD}) \qquad (2)$$

101   Equation 2 includes a scaling factor (Pechony and Shindell, 2009) originally introduced to calibrate the

102   number of fires to MODIS observations. Assuming no suppression for the first two ignition modes

103   ($f_{NS} = 1$), total ignitions (I_T, in units, ignitions $\mathrm{m}^{-2}\,\mathrm{s}^{-1}$) can be represented as (Eq. 3):

104    $$I_T = (I_N + I_A)\, f_{NS}/(8.64 \times 10^{10}) \qquad (3)$$

105   Dividing by 8.64×10^{10} converts ignitions $\mathrm{km}^{-2}\,\mathrm{month}^{-1}$ to ignitions $\mathrm{m}^{-2}\,\mathrm{s}^{-1}$.

106   **2.1.2 Flammability (F)**

107   We adapt the (Pechony and Shindell, 2009) scheme for flammability to function interactively within an

108   ESM (see Eq. 6). Starting from the saturation vapour pressure (e^*, Eq. 4; Goff and Gratch, 1946) and

109   its temperature dependence, we introduce a Fuel Density index (FD_{PFT}, Eq. 5) as well as Relative

110   Humidity (RH), precipitation and soil moisture in order to obtain Flammability (Eq. 6). The land surface

111   model (JULES) determines soil moisture content (θ) and fuel density (FD).

112    $$\log_{10}(e^*) = a\left(\frac{T_s}{T} - 1\right) + b\log_{10}\left(\frac{T_s}{T}\right) + c\left(10^{d\left(1-\frac{T_s}{T}\right)} - 1\right) + f\left(10^{h\left(\frac{T_s}{T}-1\right)} - 1\right) \qquad (4)$$

113   As illustrated in Eq. 4, INFERNO utilizes temperature (T in K, at 1.5 m height). The Goff-Gratch (Eq.

114   4) uses the constants: $a = -7.90298$; $b = 5.02808$; $c = -1.3816 * 10^{-7}$; $d = 11.344$; $f = 8.1328 *$

115   10^{-3}; $h = -3.49149$ and the water boiling point temperature $T_s = 373.16$ K.

116    $$FD_{PFT} = \begin{cases} 1 & \text{for } Fuel_{high} < (DPM_C + Leaf_{C,PFT}) \\ \frac{(DPM_C + Leaf_{C,PFT})}{Fuel_{high} - Fuel_{low}} & \text{for } Fuel_{low} < (DPM_C + Leaf_{C,PFT}) < Fuel_{high} \\ 0 & \text{for } Fuel_{low} > (DPM_C + Leaf_{C,PFT}) \end{cases} \qquad (5)$$

117   Equation 5 shows FD is taken as the PFT-specific leaf carbon ($Leaf_{C,PFT}$) plus the carbon within

118   decomposable plant material (DPM_C). DPM is a soil carbon pool of which we assume 70% is available

119   to fires i.e. near-surface (DPM is shared across all PFTs). FD scales linearly between 0 (at a threshold

120   of $Fuel_{low} = 0.02$ kgC m^{-2}) and 1 (at a threshold of $Fuel_{high} = 0.2$ kgC m^{-2}). Similar approaches to

Geoscientific
Model Development
Discussions

121   represent fuel availability within fire parameterizations have commonly been adopted (Arora and Boer,

122   2005; Li et al., 2012; Thonicke et al., 2010).

123   $F_{PFT} = e^* \left(RH_{up} - RH \right) / \left(RH_{up} - RH_{low} \right) e^{-2R} FD_{PFT} \left(1 - \theta \right)$ (6)

124   RH is the relative humidity (%) and R is the precipitation rate (mm day^{-1}). The influence of relative

125   humidity (RH) scales between (and is bound by): 0 (at a threshold of $RH_{low} = 10\%$) and 1 (at a threshold

126   of $RH_{up} = 90\%$). We then adapt the formula by replacing a vegetation index dependent on leaf area

127   index with the Fuel Density index (FD). Finally, Flammability (F_{PFT}) is dependent on upper-level (down

128   to 0.1 m) soil moisture: θ is the unfrozen soil moisture as a fraction of saturation. The individual

129   importance of these variables to our model is illustrated in Fig. A1.

2.1.3 Burnt Area (BA)

131   Our approach is to associate an average burnt area per fire to each PFT, effectively decoupling the fire-

132   spread stage from local meteorology and topography, which is typically not resolved in the relatively

133   coarse grid of an ESM. An average burnt area ($\overline{BA_{PFT}}$) was heuristically determined for each PFT: 0.6,

134   1.4 and 1.2 km^2 for trees, grass and shrubs, respectively, such that grass and shrubs will fuel larger fires

135   than trees. Observational evidence supports that the land cover type is an efficient way to characterize

136   fires, which tend to be larger in grasslands than in forests (Chuvieco et al., 2008; Giglio et al., 2013).

137   The BA is then calculated following Eq. 7:

138   $BA_{PFT} = I_T F_{PFT} \overline{BA_{PFT}}$ (7)

139   Here BA_{PFT} is the burnt area (fraction of PFT cover burnt per second) for each PFT; meanwhile the

140   number of ignitions times the flammability ($I_T F_{PFT}$) represents the number of fires.

141   Inferring burnt area from number of fires in this manner stands out from other fire models which utilize

142   wind speed (Arora and Boer, 2005; Thonicke et al., 2010; Li et al., 2012), effectively modelling the fire

143   rate of spread. Wind is key to the modelling of individual fires; yet implementing wind effectively within

144   fire models designed for the relatively coarse grid of ESMs was found to be problematic (Lasslop et al.,

145   2014, 2015). Conversely, Hantson et al. (2014) found global fire size was mostly influenced by

146   precipitation, aridity and human activity (population density and croplands).

2.1.4 Emitted Carbon (EC)

148   To account for the wetness of fuel in INFERNO, combustion completeness (the fraction of biomass

149   exposed to a fire that was volatized) scales linearly with soil moisture (as a fraction of saturation) with

150   different upper and lower boundaries for leaf and stem carbon.

151   $EC_{PFT} = BA_{PFT} \sum_{leaf,stem}^{i} \left(CC_{min,i} + \left(CC_{max,i} - CC_{min,i} \right) (1 - \theta) \right) C_i$ (8)

152   Equation 8 shows how the PFT-specific emitted carbon (EC, in kgC m^{-2} s^{-1}) is computed. BA is the burnt

153   area (fraction s^{-1}), CC_{min} and CC_{max} are the minimum and maximum combustion completeness for both

154   leaves ($CC_{min} = 0.8$ and $CC_{max} = 1.0$) and stems ($CC_{min} = 0.8$ and $CC_{max} = 1.0$), C_i is the carbon

155   stored in each PFT's leaves or stems (kgC m^{-2}). The parameters used for combustion completeness

156   (CC_{min} and CC_{max}) are similar to the Global Fire Emission Database (GFED(van der Werf et al., 2010),

157   albeit with lower minimum combustion of stems (0.0 as opposed to 0.2). This change is justifiable by

Geoscientific
Model Development
Discussions

158   the difference in the moisture used. Indeed GFED uses a more complex representation of moisture across

159   multiple fuel types, while our scheme only relies on soil moisture.

160   **2.1.5 Emitted Species (E_X)**

161   There has been a significant amount of work on estimating emission factors (EFs) across fire biomes

162   (such as savannahs, boreal forest etc.). This was synthesized in Akagi et al. (2011) as well as Andreae

163   and Merlet (2001) and its updates. To convert these biome-specific EFs to PFT specific EFs, each PFT

164   was linked to a fire biome (see Table A1). INFERNO uses these to estimate emissions (Eq. 9).

165    $E_{X,PFT} = EC_{PFT} \; EF_{X,PFT} \; /[C]$ (9)

166   Here E_X is the amount of species X emitted by fires (in kg m^{-2} s^{-1}), EC is the emitted carbon (in kgC m^{-2}

167   s^{-1}) and EF_X is the PFT-specific emission factor (see Table 1) (in kg of species emitted per kg of biomass

168   burnt), and $[C]$ is the dry biomass carbon content, express as a percentage (Lamlom and Savidge, 2003).

169   INFERNO currently provides emissions for basic trace gases: CO_2, CO, CH_4, NO_x, SO_2 and aerosols:

170   organic carbon (OC) and black carbon (BC).

171   **Table 1. INFERNO's emission factors per PFT created from the emission profiles in Akagi et al. (2011), such**
172   **that each PFT was attributed a fire biome (see Suppl. 2). This method of attributing emission factors to PFTs**
173   **is similar to that presented in Thonicke et al. (2010), and can be extended to include all species of trace gases**
174   **and aerosols compiled in Akagi et al. (2011).**

Emission Factors (g / kg)	CO_2	CO	CH_4	NO_x	SO_2	OC	BC
Broadleaf Evergreen Tree (Tropical)	1643	93	5.07	2.55	0.40	4.71	0.52
Broadleaf Evergreen Tree (Temperate)	1637	89	3.92	2.51	0.40*	8.2**	0.56**
Broadleaf Deciduous Tree	1643	93	5.07	2.55	0.40	4.71	0.52
Needleleaf Evergreen Tree	1637	89	3.92	2.51	0.40*	8.2**	0.56**
Needleleaf Deciduous Tree	1489	127	5.96	0.90	0.40*	8.2**	0.56**
C3 grass	1637	89	3.92	2.51	0.40*	8.2**	0.56**
C4 grass	1686	63	1.94	3.9	0.48	2.62	0.37
Evergreen Shrub	1637	89	3.92	2.51	0.40*	8.2**	0.56**
Deciduous Shrub	1489	127	5.96	0.90	0.40*	8.2**	0.56**

175   *Profile not available in Akagi et al. (2011), therefore we mimic tropical forests; **from Andreae and Merlet (2001).

176   **2.2 Implementation within JULES**

177   INFERNO is currently implemented within the Joint UK Land Environment Simulator (JULES). (Best

178   et al., 2011; Clark et al., 2011) its carbon fluxes and vegetation dynamics. The results shown here used

179   JULES v4.3.1 and INFERNO will be included in JULES from version 4.5 onwards. INFERNO utilizes

180   soil moisture (see Eq. 6,8) which JULES calculates as the balance between precipitation (following the

Geoscientific
Model Development
Discussions

181   scheme for rainfall interception in (Johannes Dolman and Gregory, 1992)) and extraction by

182   evapotranspiration and runoff (Cox et al. 1999; Best et al. 2011). JULES has four soil layer, and

183   INFERNO uses the top layer unfrozen soil moisture (0 to 0.1 m depth). Note that in its current state,

184   JULES does not associate carbon pools with depths, hence it is not possible to access the top-most DPM

185   only for example. The vegetation dynamics and litter carbon used obey the TRIFFID DGVM (Cox,

186   2001).

187   In JULES, vegetation carbon content is determined by the balance between photosynthesis, respiration,

188   and litterfall. Within JULES, TRIFFID (the Top-down Representation of Foliage and Flora Including

189   Dynamics; Cox et al., 2001) predicts changes in biomass and the fractional coverage of nine plant

190   functional types (Table A1) based on accumulated carbon fluxes and height-based competition, where

191   the tallest trees have the first access to space (Harper et al. *In Prep*). Vegetation can grow in height, and

192   the carbon in leaves, roots, and wood is related allometrically to the "balanced LAI", L_b (Cox et al. 2001).

193   L_b is the seasonal maximum leaf area index (LAI) and a function of plant height. Within INFERNO, leaf

194   carbon ($Leaf_C$, used for calculating FD and emissions) is:

195   $Leaf_C = \sigma_l L_b$ (10)

196   Meanwhile, wood carbon ($Wood_C$, which affects emissions), is calculated as:

197   $Wood_C = a_{wl} L_b^{b_{wl}}$ (11)

198   PFT dependent parameters(σ_l, the Specific Leaf Density, a_{wl}, the allometric coefficient and b_{wl}, the

199   allometric exponent) are given in Table A1.

200   When using JULES in its standalone version, INFERNO can use inputs of population density (in people

201   km^{-2}) and cloud-to-ground lightning flash rates (in flashes km^{-2} month^{-1}) from ancillary datasets.

202   Similarly, meteorology needs to be prescribed and is then interpolated from its native temporal resolution

203   to the model's time-step. Although designed to be integrated within an ESM, the capability to run

204   INFERNO with JULES only is particularly useful for present-day comparison with observations, and to

205   dissociate causes of biases in results.

206   **2.3 Fire Weather Indices**

207   Three other well-established daily fire indices are also available within JULES. These indices have been

208   used for several decades to help plan operational response to wildfires on Numerical Weather Predictions

209   (NWP) timescales. Although unit-less and ill-defined risk-based quantities, comparison to INFERNO is

210   still useful for understanding the results in the context of practically established metrics.

211   The Canadian Fire Weather Index (Forestry Canada, 1992; Van Wagner and Pickett, 1985) consists of

212   six components, calculated from basic meteorological parameters. Three are fuel moisture codes

213   designed to represent the drying of different fuel types, their characteristics are displayed in Table A2.

214   Two intermediate quantities, the Initial Spread Index and the build-up index are calculated from these,

215   and are in turn used to yield the final Fire Weather Index.

216   The McArthur Forest Fire Danger Index (Noble et al., 1980; Sirakoff, 1985) was developed for use in

217   Australia. Simpler in its formulation than the Canadian index, it consists of a drought component

218   modified by the local temperature, humidity and wind speed. The calculation of the drought component

219 depends on the soil moisture deficit (the amount of water needed to restore the soil moisture content of
220 the top 800 mm of soil to 200 mm), which is related to the JULES soil moisture.
221 Finally, the Nesterov Index (Nesterov, 1949) is the simplest fire index implemented in JULES. It uses
222 only the daily mean temperature, mean daily dew point (or suitable substitute), daily total precipitation
223 and the previous day's index. The index is incremented daily, unless daily precipitation exceeds 3 mm,
224 in which case it is reset. The Nesterov index is a key component for other fire models (Venevsky et al.,
225 2002; Thonicke et al., 2010).

226 **3 Model configuration**

227 Monthly lightning data was obtained from LIS-OTD (Lightning Imaging Sensor-Optical Transient
228 Detector) observations for 2013 (Christian et al., 2003) and was recycled for every year in the simulation.
229 These detections were converted to cloud-to-ground strikes using the relationship presented in (Prentice
230 and Mackerras, 1977). Land use and population density were obtained from the HYDE dataset (Hurtt et
231 al., 2011) and then linearly interpolated to create inter-annually varying data. Finally annual CO_2
232 concentrations, which affect vegetation dynamics, were prescribed as a global average following the
233 dataset prepared for the global carbon budget (Le Quéré et al., 2015).
234 To test the sensitivity to the meteorological input, JULES simulations were driven by meteorology from
235 both CRU-NCEP (Climate Research Unit and -National Center for Environmental Prediction) v5
236 (http://dods.extra.cea.fr/data/p529viov/cruncep/), and WFDEI (Weedon et al., 2014) with precipitation
237 from the GPCC (Schneider et al., 2013). Both datasets were used on a 6-hourly basis.
238 Outside of these driving variables, JULES was configured according to the TRENDY project (Sitch et
239 al., 2015)(Peng et al., 2015)(Peng et al., 2015). 100 year spin-up was performed repeating the 1990-2000
240 conditions tenfold. Four configurations were used to create simulations covering 1990-2013, although to
241 validate INFERNO only the 1997-2010 period was analysed. The first three use CRU-NCEP
242 meteorology with each of our three ignitions modes (see Sect. 2.1.1); constant ignitions (mode 1),
243 prescribed lightning and constant anthropogenic ignitions (mode 2), and both natural and anthropogenic
244 ignitions varying with prescribed lightning and population density (mode 3). The fourth simulation
245 assumes mode 1 (constant ignitions), while meteorology is prescribed from WFDEI and precipitation
246 from GPCC.

247 **4 Results**

248 Maps of the burnt area and emitted carbon are displayed in Fig. 2, their resolution is 192 longitudes by
249 145 latitudes grid-cells (1.875^ox1.24^o). The results from INFERNO used a configuration with CRUNCEP
250 meteorology and the third ignition mode: interactive lighting and anthropogenic ignitions. We compare
251 our results with downscaled means from GFED. Note GFEDv4s' burnt area (http://globalfiredata.org,
252 manuscript in preparation) differs from GFEDv4's (Giglio et al., 2013) as it includes small fires
253 (Randerson et al., 2012). Over the total study period, INFERNO diagnoses accurate global fire
254 occurrence and emissions (with R=0.66 for burnt area and R=0.59 for emitted carbon). In addition,
255 regional mean yearly budgets are compared with GFED in Table B1. We notice burnt area is higher in

256   all regions other than Australia and New Zealand, and southern hemisphere Africa. Meanwhile emitted

257   carbon is underestimated in boreal regions and equatorial Asia, but overestimated in most other regions

258   (significantly in southern hemisphere America). GFEDv4 observes the grid-box with maximum burnt

259   area within the Central African Republic (87% of grid fraction burnt per year), while INFERNO finds a

260   maximum burnt area of 57%, slightly to the North (south-east of lake Tchad). The discrepancy is much

261   larger for emissions, with a maximum emitted carbon of 1.47 kg per m^2 in Indonesia predicted by

262   GFEDv4s, against 0.4 kg per m^2 for INFERNO, in Angola. These results could be expected, as

263   INFERNO focuses on capturing global biomass burning, it will not represent such extremes of burning,

264   furthermore the immense emitted carbon observed in Indonesia follows from undiagnosed peat fires.
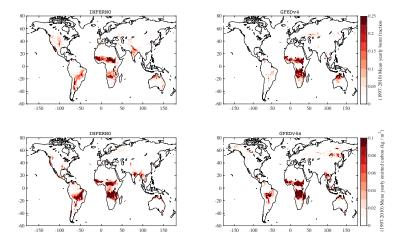

265

Fig. 2. 1997-2010 mean yearly burnt fraction (above) and emitted carbon (below, in kg m^{-2}). Shown for INFERNO on the left (with CRUNCEP meteorology and interactive ignitions: mode 3) and for GFED on the right.

269   Figure 3 shows the modelled global annual average biomass burning emissions and burnt area from 1997

270   to 2010. The three ignition methods are evaluated: fully interactive ignitions (red) predict the highest

271   carbon emissions while interactive lightning with constant human ignitions (blue) the lowest. WFDEI

272   was observed to lead to more biomass burning emissions in tropical forest areas (and in particular the

273   borders of rainforests), while CRU-NCEP favoured burning in near-desert areas (the Sahel, India and

274   south American grasslands). We expect this result to be significantly influenced by differences in

275   precipitation (GPCC for WFDEI runs and CRU for CRU-NCEP; (Schneider et al., 2013).

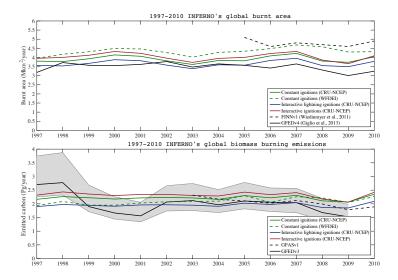Geoscientific
Model Development
Discussions

276

Fig. 3. 1997-2010 biomass burning emissions and burnt area predicted by INFERNO. Two driving datasets were used, CRU-NCEP (solid lines) and WFDEI (green dotted line). Observations are shown in black (MODIS-based estimates).

Comparisons with GFASv1 (and GFEDv3 for emissions (the grey shading represents one standard deviation within GFEDv3's estimates), to FINNv1 and GFEDv4 for burnt area, were restricted to their budgets published in (Kaiser et al., 2012; van der Werf et al., 2010; Wiedinmyer et al., 2011; Giglio et al., 2013) respectively. We also calculated global emissions from GFEDv4s (http://globalfiredata.org, manuscript in preparation), which adds a small fire contribution (Randerson et al., 2012) to GFEDv4's burnt area.

Biomass burning emissions and burnt area simulated by the model follow similar trends to GFEDv3, although with a smaller inter-annual variability in the model. Carbon emissions from all simulations fall within one standard deviation of GFEDv3, apart from three years: 1997, 1998 and 2001. Note that for these years, emissions in GFED were obtained from the lower resolution AVHRR rather than MODIS. 1997 and 1998 were strong El-Niño years during which droughts in equatorial Asia led to extreme emissions from land-clearing fires, a recurrent problem in the region (Field et al., 2009). Indeed in 1997, in the region contained between 20S-20N and 90E-160E (or equatorial Asia), GFEDv3 estimate emissions of 1.07 PgC, while INFERNO (with CRU-NCEP and fully interactive ignitions) estimates 0.15 PgC. Unfortunately, peat is not modelled in JULES and thus neither is peat present in our fire scheme. It was estimated tropical peat fires alone produced an average of 0.1 PgC per year for 1997-2009, and 0.7 PgC in 1997 in particular (van der Werf et al., 2010). Peat-lands can be significant in equatorial Asia but also boreal regions where their combustion leads to the release of long-stored carbon (Turetsky et al., 2015). In 1998 and 2001, the difference in emissions could not be attributed to a particular location. While fire emissions from Equatorial Asia were underestimated, GFEDv3 observed lower emissions over Africa compared to INFERNO, which seems to be the key driver of our discrepancies.

Table 2. Mean yearly emission budgets in Peta-grams of emitted carbon and mean yearly burnt area budgets in Mkm2 for the 1997-2010 period. Latitudes were bound to: beyond 50º (high latitudes), 35º to 50º (mid-

Geoscientific
Model Development
Discussions

304   latitudes), 15º to 35º (low latitudes) and below 15º (equatorial). Four configurations of INFERNO are
305   presented, with CRU-NCEP and WFDEI driving meteorology coupled with three ignition modes: mode 1
306   indicates constant anthropogenic and lightning ignitions, mode 2 is for constant anthropogenic with
307   interactive lightning ignitions, and mode 3 for interactive lightning and anthropogenic ignitions.

Emitted carbon (PgC/year)	mode 1 CRU-NCEP	mode 1 WFDEI	mode 2 CRU-NCEP	mode 3 CRU-NCEP
High latitudes	0.087	0.096	0.082	0.091
Mid-latitudes	0.185	0.193	0.170	0.191
Low latitudes	0.716	0.624	0.627	0.591
Equatorial	1.157	1.130	1.021	1.385

308

Burnt area (Mkm^2 / year)	mode 1 CRU-NCEP	mode 1 WFDEI	mode 2 CRU-NCEP	mode 3 CRU-NCEP
High latitudes	0.176	0.196	0.162	0.179
Mid-latitudes	0.485	0.557	0.445	0.531
Low latitudes	1.648	1.884	1.558	1.531
Equatorial	1.524	1.580	1.423	1.693

309

310   Table 2 shows the budgets for four latitudinal bands across the various simulations performed. The

311   second ignition mode (constant anthropogenic and interactive lightning ignitions at any time and place)

312   appears to consistently predict lower emissions and burnt area (with the exception of low latitudes).

313   Furthermore, the main impact of using an ignition model that varies with both natural and anthropogenic

314   ignitions is a reduction of fires at low (tropical and sub-tropical) latitudes, and an increase in equatorial

315   regions. Indeed, when compared to constant ignitions (mode 1), interactive ignitions (mode 3) predict

316   more emissions in forest encroachment regions (noticeably surrounding the Congo and Amazon

317   rainforests), and less in heavily-populated areas (Nigeria, India). Meanwhile, we observed interactive

318   lightning ignitions (mode 2) significantly reduced burning in grassland-savannah environments. We link

319   this to the predominance of cloud-to-ground lightning strikes in wet environment within the LIS-OTD

320   dataset (e.g. the Congo rainforest, (Christian et al., 2003) and fewer strikes (and ignitions) in the more

321   flammable grasslands and savannahs. These issues are visible in Fig. B1, which shows difference maps

322   of the four model configurations, for 1997-2010 mean yearly totals. Equatorial and boreal regions include

323   peat that leads to large fuel consumption, which is unaccounted for in JULES, suggesting that our model

324   will inherently underestimate emissions from these regions.

325   In order to examine whether our flammability can represent fire occurrence, three other fire indices were

326   diagnosed, namely the McArthur, Nesterov and Canadian fire indices. These indices were obtained

327   seamlessly during the model runs, therefore utilizing the same meteorological and hydrological driving

328   variables, and the same vegetation condition. Their predictions were regressed with GFEDv4 1997-2010

Geoscientific
Model Development
Discussions

329 annual burnt area (Giglio et al., 2013). This analysis relies on the assumption that fire indices can be used

330 as a proxy for fire occurrence and spread, and eventually burnt area. Only areas that had been observed

331 to burn sometime between 1997 and 2010 were sampled; to avoid accounting for high fire indices in

332 non-vegetated areas such as the Sahara.

333 Table 3 shows the result of our analysis. Ignitions followed mode 1; in this mode ignitions are constant,

334 therefore the only variability in burnt area (and performance) is due to INFERNO's flammability scheme.

335 The McArthur index performs poorly at high latitudes (it was made for Australia), but outperforms the

336 other indices in low latitude regions. The Canadian and Nesterov indices correlate best with observed

337 burnt area in high latitude regions (for which they were developed). Altogether, INFERNO's burnt area

338 appears to follow observed burnt area better than the sole usage of a fire index.

339 **Table 3. Temporal correlation coefficients (R) of annual means (1997-2010) shown for four latitudinal bands.**
340 **R-coefficients were obtained between either of the three simulated fire indices or INFERNO's burnt area**
341 **(ubiquitous ignitions – ignition mode 1, using CRU-NCEP meteorology) and burnt area from GFEDv4 (Giglio**
342 **et al., 2013). We restrict our analysis to grid-boxes in which GFEDv4 observed burning. Latitudes were bound**
343 **to: beyond 50° (high latitudes), 35° to 50° (mid-latitudes), 15° to 35° (low latitudes) and below 15° (equatorial).**

R-coefficient (with GFEDv4 burnt area)	INFERNO Burnt area	Nesterov Index	McArthur Index	Canadian Index
Global	0.649	0.088	-0.009	0.266
High latitudes	0.476	0.522	-0.005	0.519
Mid-latitudes	0.179	-0.006	0.069	0.060
Low latitudes	0.603	0.476	0.499	0.480
Equatorial	0.689	0.239	0.354	0.392

344

5 Conclusion

346 Through a minimalistic approach we propose a parameterization for fire occurrence of appropriate

347 complexity for application at large spatial scales within an ESM context: the INteractive Fire and

348 Emission algoRithm for Natural envirOnments (INFERNO). It directly only varies according to

349 precipitation (and resulting soil moisture), temperature and humidity, and indirectly it utilizes vegetation.

350 It is also capable of explicitly simulating ignitions using lightning and anthropogenic information. While

351 our scheme manages to represent fire occurrence on large scales (both spatial and temporal), it performs

352 best at low latitudes. INFERNO's burnt area scheme appears superior to the use of fire indices alone

353 (Nesterov, McArthur and basic Canadian) for capturing annual burnt area variations, and thus one form

354 of fire impact. However, due to the nature of our analysis (fire danger and burnt area remain different

355 quantities) this does not imply INFERNO should supersede fire weather indices for operational purposes,

356 neither has our algorithm been built for numerical weather prediction or seasonal fire danger forecasting.

357 Nonetheless, our current simulations suggest the variability in emissions is underestimated by

358 INFERNO, in particular the impact of the 1997-1998 El-Niño and the subsequent La Niña, which may

359   be attributable to the lack of representation of peat in the model, critical to biomass burning in equatorial

360   Asia and boreal areas. The use of different present-day meteorological datasets, in particular

361   precipitation, has an important impact on the magnitude and variability of our diagnostics. Using

362   WFDEI-GPCC rather than CRU-NCEP led to more burnt area but lower fuel consumption and eventually

363   less emitted carbon (this follows from grasslands burning rather than forests). Vegetation zone interfaces

364   were key to this difference. Similarly, lightning appears to ignite more fires in wet environments

365   (rainforests) while flammable environments (savannah, grasslands) are sensitive to the presence of an

366   ignition source. Including a scheme to parameterise human impacts appears to significantly reduce fires

367   in heavily populated areas, while favouring their encroachment of rainforests (the vicinity of which are

368   an anthropogenic ignition 'sweet spot' in our parameterization). Nevertheless there is much uncertainty

369   attributed to human induced emissions and effects on fire regime (Marlon et al., 2008; Thonicke et al.,

370   2010). Accordingly, we include different modes of ignition to dampen the impact of this uncertainty in

371   INFERNO.

372   The implementation of INFERNO within the Met Office's Unified Model and its significance for

373   present-day atmospheric composition and climate will be investigated in a separate paper. While a

374   strength of the model is its minimalistic approach the scheme holds potential for improvements: while

375   litter influences flammability, only live vegetation is vaporized. In reality, litter is observed to burn more

376   than live vegetation. Similarly, we predict that the inclusion of peat within JULES would improve its fire

377   diagnostics, especially for locations with large fuel consumptions (e.g. equatorial Asia and boreal

378   climates; van der Werf et al., 2010). Given the predictability of emissions from peat fires in relation with

379   precipitation (van der Werf et al., 2008), this would be a promising area of exploration. The value of this

380   model being its simplicity and linearity, any improvements to INFERNO's meteorological and

381   hydrological assimilation need to remain minimalistic; complex parameterizations are better suited for

382   more specialized fire schemes (Lasslop et al., 2014; Li et al., 2013, p.1).

383   **Code availability**

384   Information on the JULES land surface model can be found at: http://jules-lsm.github.io/. INFERNO is

385   included in JULES vn4.5 and is included in this documentation. The JULES source code can be accessed

386   via the Met Office's science repository (requires registration): https://code.metoffice.gov.uk/trac/jules.

387   In particular, the version of the code used to produce the outputs included in this study can be accessed

388   at:

389   https://code.metoffice.gov.uk/trac/jules/browser/main/branches/dev/stephanemangeon/vn4.3.1_inferno.

390   **Appendix A**

391   This appendix contains additional information relating to the INFERNO scheme.
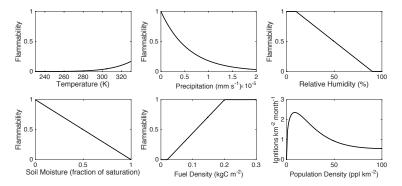
392

Fig. A1. The individual dependencies of INFERNO on key driving variables. Note the population density only influences the model output if ignition mode 3 is selected (interactive lightning and human ignition).

393
394

395 **Table A1. The key JULES PFT-specific parameters for allometry and vegetation carbon used in our**
396 **simulations (Clark et al., 2011).**

	Specific leaf density σ_l (kg C m^{-2})	Allometric coefficient a_{wl} (kg C m^{-2})	Allometric exponent b_{wl}	Associated Fire Biome in Akagi et al., 2011
Broadleaf Evergreen Tree (Tropical)	0.0375	0.65	1.667	Tropical Forests
Broadleaf Evergreen Tree (Temperate)	0.0375	0.65	1.667	Temperate Forests
Broadleaf Deciduous Tree	0.0375	0.65	1.667	Tropical Forests
Needleleaf Evergreen Tree	0.1	0.65	1.667	Temperate Forests
Needleleaf Deciduous Tree	0.1	0.75	1.667	Boreal Forests
C3 grass	0.025	0.005	1.667	Temperate Forests
C4 grass	0.05	0.005	1.667	Savannah and Grasslands
Evergreen Shrub	0.05	0.10	1.667	Temperate Forests
Deciduous Shrub	0.05	0.10	1.667	Boreal Forests

397

398 **Table A2. The characteristics of the Canadian's Fire Weather Index's three fuel moisture codes.**

	Type of fuel	Dry weight (kg m^{-2})	Time lag (days)	Water capacity (mm)
Fine Fuel Moisture Code	Litter and other fine fuels	0.25	2-3	0.6
Duff Moisture Code	Loosely compacted decomposing organic matter	5	12	15

Drought Code	Deep layer of compact organic matter	25	52	100

399 **Appendix B**

400 This appendix contains additional results illustrating the dependence of INFERNO with ignitions and its
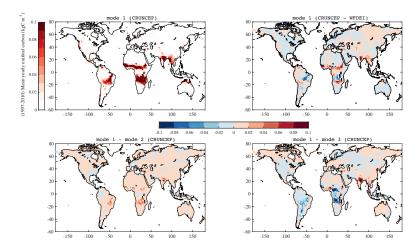
401 performance on a regional basis.

402

403 **Fig. B1. Emitted carbon difference maps between the four runs performed to analyse the sensitivity of**
404 **INFERNO to ignitions (our three ignition modes, see Sect. 2.1.1) and meteorology (CRUNCEP and WFDEI-**
405 **GPCC).**

406 **Table B1. Regional budgets according to the standard GFED regions (van der Werf et al., 2010).**

GFED standard regions	Mean Yearly Burnt Area (in Mha)		Mean Yearly Emitted Carbon (in TgC)	
	GFED4*	INFERNO**	GFED3***	INFERNO**
Boreal North America	2.2	5.2	54	37
Temperate North America	1.8	29.9	9	106
Central America	1.8	7.9	20	45
Northern Hemisphere South America	2.6	4.0	22	51
Southern Hemisphere South America	18.7	68.3	271	483
Europe	0.7	5.0	4	29
Middle East	0.8	12.3	2	19

Northern Hemisphere Africa	117.7	120.4	481	533
Southern Hemisphere Africa	125.0	57.6	557	610
Boreal Asia	5.6	9.7	128	55
Central Asia	13.6	23.8	36	50
Southeast Asia	7.0	29.6	103	170
Equatorial Asia	1.6	0.5	191	10
Australia and New Zealand	50.2	30.2	135	96

407 * GFED4 mean yearly burnt area from Giglio et al. (2013), from 1997 to 2011. ** INFERNO mean yearly burnt area from 1997

408 to 2010, using ignition mode 3 (varying anthropogenic and natural ignitions) and CRU-NCEP driving meteorology. *** GFED3

409 mean yearly emitted carbon from van der Werf et al. (2010) from 1997 to 2009.

Geoscientific Model Development
Discussions

Open Access

EGU

Author contribution

Apostolos Voulgarakis supervised the scientific design of INFERNO and the writing of this article. Gerd Folberth also supervised these aspects, with an emphasis on technical aspects of INFERNO in relation with the Met Office's Unified Model. Richard Gilham contributed to the technical design of the model and its implementation and led the writing on fire indices. Anna Harper contributed to the design of INFERNO in relation to the vegetation scheme's recent development, helped with the analysis of vegetation biases in the study's results and led the writing on the vegetation scheme. Stephen Sitch contributed throughout the writing, analysis and the scientific design of this study.

Acknowledgements

References

Akagi, S. K., Yokelson, R. J., Wiedinmyer, C., Alvarado, M. J., Reid, J. S., Karl, T., Crounse, J. D. and Wennberg, P. O.: Emission factors for open and domestic biomass burning for use in atmospheric models, Atmos Chem Phys, 11(9), 4039–4072, doi:10.5194/acp-11-4039-2011, 2011.

Arora, V. K. and Boer, G. J.: Fire as an interactive component of dynamic vegetation models, J. Geophys. Res. Biogeosciences, 110(G2), G02008, doi:10.1029/2005JG000042, 2005.

Best, M. J., Pryor, M., Clark, D. B., Rooney, G. G., Essery, R. . L. H., Ménard, C. B., Edwards, J. M., Hendry, M. A., Porson, A., Gedney, N., Mercado, L. M., Sitch, S., Blyth, E., Boucher, O., Cox, P. M., Grimmond, C. S. B. and Harding, R. J.: The Joint UK Land Environment Simulator (JULES), model description – Part 1: Energy and water fluxes, Geosci. Model Dev., 4(3), 677–699, doi:10.5194/gmd-4-677-2011, 2011.

Bond, W. J. and Keeley, J. E.: Fire as a global "herbivore": the ecology and evolution of flammable ecosystems, Trends Ecol. Evol., 20(7), 387–394, doi:10.1016/j.tree.2005.04.025, 2005.

Bowman, D. M., Murphy, B. P., Boer, M. M., Bradstock, R. A., Cary, G. J., Cochrane, M. A., Fensham, R. J., Krawchuk, M. A., Price, O. F. and Williams, R. J.: Forest fire management, climate change, and the risk of catastrophic carbon losses, Front. Ecol. Environ., 11(2), 66–67, doi:10.1890/13.WB.005, 2013.

Bowman, D. M. J. S., Balch, J. K., Artaxo, P., Bond, W. J., Carlson, J. M., Cochrane, M. A., D'Antonio, C. M., DeFries, R. S., Doyle, J. C., Harrison, S. P., Johnston, F. H., Keeley, J. E., Krawchuk, M. A., Kull, C. A., Marston, J. B., Moritz, M. A., Prentice, I. C., Roos, C. I., Scott, A. C., Swetnam, T. W., Werf, G. R. van der and Pyne, S. J.: Fire in the Earth System, Science, 324(5926), 481–484, doi:10.1126/science.1163886, 2009.

Christian, H. J., Blakeslee, R. J., Boccippio, D. J., Boeck, W. L., Buechler, D. E., Driscoll, K. T., Goodman, S. J., Hall, J. M., Koshak, W. J., Mach, D. M. and Stewart, M. F.: Global frequency and

449 distribution of lightning as observed from space by the Optical Transient Detector, J. Geophys. Res.
450 Atmospheres, 108(D1), 4005, doi:10.1029/2002JD002347, 2003.

451 Chuvieco, E., Giglio, L. and Justice, C.: Global characterization of fire activity: toward defining fire
452 regimes from Earth observation data, Glob. Change Biol., 14(7), 1488–1502, 2008.

453 Clark, D. B., Mercado, L. M., Sitch, S., Jones, C. D., Gedney, N., Best, M. J., Pryor, M., Rooney, G. G.,
454 Essery, R. L. H., Blyth, E., Boucher, O., Harding, R. J., Huntingford, C. and Cox, P. M.: The Joint UK
455 Land Environment Simulator (JULES), model description – Part 2: Carbon fluxes and vegetation
456 dynamics, Geosci Model Dev, 4(3), 701–722, doi:10.5194/gmd-4-701-2011, 2011.

457 Cox, P. M.: Description of the TRIFFID dynamic global vegetation model, Technical Note 24, Hadley
458 Centre, United Kingdom Meteorological Office, Bracknell, UK. [online] Available from:
459 http://www.metoffice.gov.uk/media/pdf/9/h/HCTN_24.pdf (Accessed 10 September 2015), 2001.

460 Field, R. D., van der Werf, G. R. and Shen, S. S. P.: Human amplification of drought-induced biomass
461 burning in Indonesia since 1960, Nat. Geosci., 2(3), 185–188, doi:10.1038/ngeo443, 2009.

462 Forestry Canada: Development and structure of the Canadian Forest Fire Behavior Prediction System.
463 [online] Available from: http://cfs.nrcan.gc.ca/publications?id=10068 (Accessed 8 January 2016), 1992.

464 Fosberg, M. A., Cramer, W., Brovkin, V., Fleming, R., Gardner, R., Gill, A. M., Goldammer, J. G.,
465 Keane, R., Koehler, P., Lenihan, J., Neilson, R., Sitch, S., Thornicke, K., Venevski, S., Weber, M. G.
466 and Wittenberg, U.: Strategy for a Fire Module in Dynamic Global Vegetation Models, Int. J. Wildland
467 Fire, 9(1), 79–84, 1999.

468 Giglio, L., Randerson, J. T. and van der Werf, G. R.: Analysis of daily, monthly, and annual burned area
469 using the fourth-generation global fire emissions database (GFED4), J. Geophys. Res. Biogeosciences,
470 118(1), 317–328, doi:10.1002/jgrg.20042, 2013.

471 Hantson, S., Pueyo, S. and Chuvieco, E.: Global fire size distribution is driven by human impact and
472 climate, Glob. Ecol. Biogeogr., n/a–n/a, doi:10.1111/geb.12246, 2014.

473 Huntrieser, H., Schumann, U., Schlager, H., Höller, H., Giez, A., Betz, H.-D., Brunner, D., Forster, C.,
474 O. Pinto Jr. and Calheiros, R.: Lightning activity in Brazilian thunderstorms during TROCCINOX:
475 implications for NOx production, Atmos Chem Phys Discuss, 7(5), 14813–14894, doi:10.5194/acpd-7-
476 14813-2007, 2007.

477 Hurtt, G. C., Chini, L. P., Frolking, S., Betts, R. A., Feddema, J., Fischer, G., Fisk, J. P., Hibbard, K.,
478 Houghton, R. A., Janetos, A., Jones, C. D., Kindermann, G., Kinoshita, T., Goldewijk, K. K., Riahi, K.,
479 Shevliakova, E., Smith, S., Stehfest, E., Thomson, A., Thornton, P., Vuuren, D. P. van and Wang, Y. P.:
480 Harmonization of land-use scenarios for the period 1500–2100: 600 years of global gridded annual land-
481 use transitions, wood harvest, and resulting secondary lands, Clim. Change, 109(1-2), 117–161,
482 doi:10.1007/s10584-011-0153-2, 2011.

483 Johannes Dolman, A. and Gregory, D.: The Parametrization of Rainfall Interception In GCMs, Q. J. R.
484 Meteorol. Soc., 118(505), 455–467, doi:10.1002/qj.49711850504, 1992.

485 Johnston, F. H., Henderson, S. B., Chen, Y., Randerson, J. T., Marlier, M., DeFries, R. S., Kinney, P.,
486 Bowman, D. M. J. S. and Brauer, M.: Estimated Global Mortality Attributable to Smoke from Landscape
487 Fires, Environ. Health Perspect., 120(5), 695–701, doi:10.1289/ehp.1104422, 2012.

488 Kaiser, J. W., Heil, A., Andreae, M. O., Benedetti, A., Chubarova, N., Jones, L., Morcrette, J.-J.,
489 Razinger, M., Schultz, M. G., Suttie, M. and van der Werf, G. R.: Biomass burning emissions estimated
490 with a global fire assimilation system based on observed fire radiative power, Biogeosciences, 9(1), 527–
491 554, doi:10.5194/bg-9-527-2012, 2012.

492 Lamarque, J.-F., Bond, T. C., Eyring, V., Granier, C., Heil, A., Klimont, Z., Lee, D., Liousse, C.,
493 Mieville, A., Owen, B. and others: Historical (1850–2000) gridded anthropogenic and biomass burning

Geoscientific
Model Development
Discussions

494   emissions of reactive gases and aerosols: methodology and application, Atmospheric Chem. Phys.,
495   10(15), 7017–7039, 2010.

496   Lamlom, S. H. and Savidge, R. A.: A reassessment of carbon content in wood: variation within and
497   between 41 North American species, Biomass Bioenergy, 25(4), 381–388, doi:10.1016/S0961-
498   9534(03)00033-3, 2003.

499   Lasslop, G., Thonicke, K. and Kloster, S.: SPITFIRE within the MPI Earth system model: Model
500   development and evaluation, J. Adv. Model. Earth Syst., n/a–n/a, doi:10.1002/2013MS000284, 2014.

501   Lasslop, G., Hantson, S. and Kloster, S.: Influence of wind speed on the global variability of burned
502   fraction: a global fire model's perspective, Int. J. Wildland Fire, 24(7), 989–1000, 2015.

503   Le Quéré, C., Moriarty, R., Andrew, R. M., Peters, G. P., Ciais, P., Friedlingstein, P., Jones, S. D., Sitch,
504   S., Tans, P., Arneth, A., Boden, T. A., Bopp, L., Bozec, Y., Canadell, J. G., Chini, L. P., Chevallier, F.,
505   Cosca, C. E., Harris, I., Hoppema, M., Houghton, R. A., House, J. I., Jain, A. K., Johannessen, T., Kato,
506   E., Keeling, R. F., Kitidis, V., Klein Goldewijk, K., Koven, C., Landa, C. S., Landschützer, P., Lenton,
507   A., Lima, I. D., Marland, G., Mathis, J. T., Metzl, N., Nojiri, Y., Olsen, A., Ono, T., Peng, S., Peters, W.,
508   Pfeil, B., Poulter, B., Raupach, M. R., Regnier, P., Rödenbeck, C., Saito, S., Salisbury, J. E., Schuster,
509   U., Schwinger, J., Séférian, R., Segschneider, J., Steinhoff, T., Stocker, B. D., Sutton, A. J., Takahashi,
510   T., Tilbrook, B., van der Werf, G. R., Viovy, N., Wang, Y.-P., Wanninkhof, R., Wiltshire, A. and Zeng,
511   N.: Global carbon budget 2014, Earth Syst. Sci. Data, 7(1), 47–85, doi:10.5194/essd-7-47-2015, 2015.

512   Li, F., Zeng, X. D. and Levis, S.: A process-based fire parameterization of intermediate complexity in a
513   Dynamic Global Vegetation Model, Biogeosciences, 9(7), 2761–2780, doi:10.5194/bg-9-2761-2012,
514   2012.

515   Li, F., Levis, S. and Ward, D. S.: Quantifying the role of fire in the Earth system – Part 1: Improved
516   global fire modeling in the Community Earth System Model (CESM1), Biogeosciences, 10(4), 2293–
517   2314, doi:10.5194/bg-10-2293-2013, 2013.

518   Li, F., Bond-Lamberty, B. and Levis, S.: Quantifying the role of fire in the Earth system – Part 2: Impact
519   on the net carbon balance of global terrestrial ecosystems for the 20th century, Biogeosciences, 11(5),
520   1345–1360, doi:10.5194/bg-11-1345-2014, 2014.

521   Marlier, M. E., DeFries, R. S., Voulgarakis, A., Kinney, P. L., Randerson, J. T., Shindell, D. T., Chen,
522   Y. and Faluvegi, G.: El Nino and health risks from landscape fire emissions in southeast Asia, Nat. Clim.
523   Change, 3(2), 131–136, doi:10.1038/nclimate1658, 2013.

524   Marlon, J. R., Bartlein, P. J., Carcaillet, C., Gavin, D. G., Harrison, S. P., Higuera, P. E., Joos, F., Power,
525   M. J. and Prentice, I. C.: Climate and human influences on global biomass burning over the past
526   two millennia, Nat. Geosci., 1(10), 697–702, doi:10.1038/ngeo313, 2008.

527   Nesterov, V.: Forest fires and methods of fire risk determination, Russ. Goslesbumizdat Mosc., 1949.

528   Noble, I. R., Gill, A. M. and Bary, G. a. V.: McArthur's fire-danger meters expressed as equations, Aust.
529   J. Ecol., 5(2), 201–203, doi:10.1111/j.1442-9993.1980.tb01243.x, 1980.

530   Pechony, O. and Shindell, D. T.: Fire parameterization on a global scale, J. Geophys. Res. Atmospheres,
531   114(D16), D16115, doi:10.1029/2009JD011927, 2009.

532   Pechony, O. and Shindell, D. T.: Driving forces of global wildfires over the past millennium and the
533   forthcoming century, Proc. Natl. Acad. Sci., doi:10.1073/pnas.1003669107, 2010.

534   Peng, S., Ciais, P., Chevallier, F., Peylin, P., Cadule, P., Sitch, S., Piao, S., Ahlström, A., Huntingford,
535   C., Levy, P., Li, X., Liu, Y., Lomas, M., Poulter, B., Viovy, N., Wang, T., Wang, X., Zaehle, S., Zeng,
536   N., Zhao, F. and Zhao, H.: Benchmarking the seasonal cycle of CO2 fluxes simulated by terrestrial
537   ecosystem models, Glob. Biogeochem. Cycles, 29(1), 2014GB004931, doi:10.1002/2014GB004931,
538   2015.

Geoscientific
Model Development
Discussions

539   Pfeiffer, M., Spessa, A. and Kaplan, J. O.: A model for global biomass burning in preindustrial time:
540   LPJ-LMfire (v1.0), Geosci Model Dev, 6(3), 643–685, doi:10.5194/gmd-6-643-2013, 2013.

541   Prentice, S. A. and Mackerras, D.: The Ratio of Cloud to Cloud-Ground Lightning Flashes in
542   Thunderstorms,   J.   Appl.   Meteorol.,   16(5),   545–550,   doi:10.1175/1520-
543   0450(1977)016<0545:TROCTC>2.0.CO;2, 1977.

544   Randerson, J. T., Chen, Y., van der Werf, G. R., Rogers, B. M. and Morton, D. C.: Global burned area
545   and biomass burning emissions from small fires, J. Geophys. Res. Biogeosciences, 117(G4), G04012,
546   doi:10.1029/2012JG002128, 2012.

547   Schneider, U., Becker, A., Finger, P., Meyer-Christoffer, A., Ziese, M. and Rudolf, B.: GPCC's new land
548   surface precipitation climatology based on quality-controlled in situ data and its role in quantifying the
549   global water cycle, Theor. Appl. Climatol., 115(1-2), 15–40, doi:10.1007/s00704-013-0860-x, 2013.

550   Sirakoff, C.: A correction to the equations describing the McArthur forest fire danger meter, Aust. J.
551   Ecol., 10(4), 481–481, doi:10.1111/j.1442-9993.1985.tb00909.x, 1985.

552   Sitch, S., Smith, B., Prentice, I. C., Arneth, A., Bondeau, A., Cramer, W., Kaplan, J. O., Levis, S., Lucht,
553   W., Sykes, M. T., Thonicke, K. and Venevsky, S.: Evaluation of ecosystem dynamics, plant geography
554   and terrestrial carbon cycling in the LPJ dynamic global vegetation model, Glob. Change Biol., 9(2),
555   161–185, doi:10.1046/j.1365-2486.2003.00569.x, 2003.

556   Sitch, S., Friedlingstein, P., Gruber, N., Jones, S. D., Murray-Tortarolo, G., Ahlström, A., Doney, S. C.,
557   Graven, H., Heinze, C., Huntingford, C., Levis, S., Levy, P. E., Lomas, M., Poulter, B., Viovy, N.,
558   Zaehle, S., Zeng, N., Arneth, A., Bonan, G., Bopp, L., Canadell, J. G., Chevallier, F., Ciais, P., Ellis, R.,
559   Gloor, M., Peylin, P., Piao, S. L., Le Quéré, C., Smith, B., Zhu, Z. and Myneni, R.: Recent trends and
560   drivers of regional sources and sinks of carbon dioxide, Biogeosciences, 12(3), 653–679, doi:10.5194/bg-
561   12-653-2015, 2015.

562   Spracklen, D. V., Logan, J. A., Mickley, L. J., Park, R. J., Yevich, R., Westerling, A. L. and Jaffe, D. A.:
563   Wildfires drive interannual variability of organic carbon aerosol in the western U.S. in summer, Geophys.
564   Res. Lett., 34(16), L16816, doi:10.1029/2007GL030037, 2007.

565   Thonicke, K., Venevsky, S., Sitch, S. and Cramer, W.: The role of fire disturbance for global vegetation
566   dynamics: coupling fire into a Dynamic Global Vegetation Model, Glob. Ecol. Biogeogr., 10(6), 661–
567   677, doi:10.1046/j.1466-822X.2001.00175.x, 2001.

568   Thonicke, K., Spessa, A., Prentice, I. C., Harrison, S. P., Dong, L. and Carmona-Moreno, C.: The
569   influence of vegetation, fire spread and fire behaviour on biomass burning and trace gas emissions:
570   results from a process-based model, Biogeosciences, 7(6), 1991–2011, doi:10.5194/bg-7-1991-2010,
571   2010.

572   Tosca, M. G., Randerson, J. T. and Zender, C. S.: Global impact of smoke aerosols from landscape fires
573   on climate and the Hadley circulation, Atmos Chem Phys, 13(10), 5227–5241, doi:10.5194/acp-13-5227-
574   2013, 2013.

575   Turetsky, M. R., Benscoter, B., Page, S., Rein, G., van der Werf, G. R. and Watts, A.: Global
576   vulnerability of peatlands to fire and carbon loss, Nat. Geosci., 8(1), 11–14, doi:10.1038/ngeo2325, 2015.

577   Van Wagner, C. E. and Pickett, T. L.: Equations and FORTRAN program for the Canadian Forest Fire
578   Weather Index System. [online] Available from: http://www.cfs.nrcan.gc.ca/publications/?id=19973
579   (Accessed 8 January 2016), 1985.

580   Venevsky, S., Thonicke, K., Sitch, S. and Cramer, W.: Simulating fire regimes in human-dominated
581   ecosystems: Iberian Peninsula case study, Glob. Change Biol., 8(10), 984–998, doi:10.1046/j.1365-
582   2486.2002.00528.x, 2002.

583   Voulgarakis, A. and Field, R. D.: Fire Influences on Atmospheric Composition, Air Quality and Climate,
584   Curr. Pollut. Rep., 1(2), 70–81, doi:10.1007/s40726-015-0007-z, 2015.

Geoscientific
Model Development
Discussions

585 Voulgarakis, A., Savage, N. H., Wild, O., Braesicke, P., Young, P. J., Carver, G. D. and Pyle, J. A.:
586 Interannual variability of tropospheric composition: the influence of changes in emissions, meteorology
587 and clouds, Atmos Chem Phys, 10(5), 2491–2506, doi:10.5194/acp-10-2491-2010, 2010.

588 Voulgarakis, A., Marlier, M. E., Faluvegi, G., Shindell, D. T., Tsigaridis, K. and Mangeon, S.:
589 Interannual variability of tropospheric trace gases and aerosols: The role of biomass burning emissions,
590 J. Geophys. Res. Atmospheres, 120(14), 7157–7173, doi:10.1002/2014JD022926, 2015.

591 Weedon, G. P., Balsamo, G., Bellouin, N., Gomes, S., Best, M. J. and Viterbo, P.: The WFDEI
592 meteorological forcing data set: WATCH Forcing Data methodology applied to ERA-Interim reanalysis
593 data, Water Resour. Res., 50(9), 7505–7514, doi:10.1002/2014WR015638, 2014.

594 van der Werf, G. R., Morton, D. C., DeFries, R. S., Olivier, J. G. J., Kasibhatla, P. S., Jackson, R. B.,
595 Collatz, G. J. and Randerson, J. T.: CO2 emissions from forest loss, Nat. Geosci., 2(11), 737–738,
596 doi:10.1038/ngeo671, 2009.

597 van der Werf, G. R., Randerson, J. T., Giglio, L., Collatz, G. J., Mu, M., Kasibhatla, P. S., Morton, D.
598 C., DeFries, R. S., Jin, Y. and van Leeuwen, T. T.: Global fire emissions and the contribution of
599 deforestation, savanna, forest, agricultural, and peat fires (1997–2009), Atmos Chem Phys, 10(23),
600 11707–11735, doi:10.5194/acp-10-11707-2010, 2010.

601 van der Werf, G., Dempewolf, J., Trigg, S. N., Randerson, J. T., Kasibhatla, P. S., Giglio, L., Murdiyarso,
602 D., Peters, W., Morton, D. C., Collatz, G. J., Dolman, A. J. and DeFries, R. S.: Climate regulation of fire
603 emissions and deforestation in equatorial Asia, Proc. Natl. Acad. Sci., 105(51), 20350–20355,
604 doi:10.1073/pnas.0803375105, 2008.

605 Wiedinmyer, C., Akagi, S. K., Yokelson, R. J., Emmons, L. K., Al-Saadi, J. A., Orlando, J. J. and Soja,
606 A. J.: The Fire INventory from NCAR (FINN): a high resolution global model to estimate the emissions
607 from open burning, Geosci. Model Dev., 4(3), 625–641, doi:10.5194/gmd-4-625-2011, 2011.

608 Yue, C., Ciais, P., Cadule, P., Thonicke, K., Archibald, S., Poulter, B., Hao, W. M., Hantson, S.,
609 Mouillot, F., Friedlingstein, P., Maignan, F. and Viovy, N.: Modelling the role of fires in the terrestrial
610 carbon balance by incorporating SPITFIRE into the global vegetation model ORCHIDEE – Part 1:
611 simulating historical global burned area and fire regimes, Geosci Model Dev, 7(6), 2747–2767,
612 doi:10.5194/gmd-7-2747-2014, 2014.

613